

# Analytical Methods

Accepted Manuscript



This is an *Accepted Manuscript*, which has been through the RSC Publishing peer review process and has been accepted for publication.

*Accepted Manuscripts* are published online shortly after acceptance, which is prior to technical editing, formatting and proof reading. This free service from RSC Publishing allows authors to make their results available to the community, in citable form, before publication of the edited article. This *Accepted Manuscript* will be replaced by the edited and formatted *Advance Article* as soon as this is available.

To cite this manuscript please use its permanent Digital Object Identifier (DOI®), which is identical for all formats of publication.

More information about *Accepted Manuscripts* can be found in the [Information for Authors](#).

Please note that technical editing may introduce minor changes to the text and/or graphics contained in the manuscript submitted by the author(s) which may alter content, and that the standard [Terms & Conditions](#) and the [ethical guidelines](#) that apply to the journal are still applicable. In no event shall the RSC be held responsible for any errors or omissions in these *Accepted Manuscript* manuscripts or any consequences arising from the use of any information contained in them.

1 **Molecularly imprinted colloidal array as a colorimetric sensor for label-free detection of**  
2 ***p*-nitrophenol**

3 Fei Xue, Zihui Meng\*, Yifei Wang, Shuyue Huang, Qihong Wang, Wei Lu, Min Xue\*

4 School of Chemical Engineering and Environment, Beijing Institute of Technology, 5  
5 Zhongguancun South Street, Beijing 100081, P. R. China

6 \*Co-corresponding author: m\_zihui@yahoo.com, minxue@bit.edu.cn, Tel & Fax:  
7 86-10-68913065

8 **Abstract**

9 We report on the synthesis of a label-free *p*-nitrophenol (PNP) responsive crystalline colloidal  
10 array (CCA) based on the combination of photonic crystal and molecular imprinting  
11 technique. This novel sensing material was prepared by a self-assembly approach using PNP  
12 imprinted colloidal spheres and was characterized by a three-dimensional (3D) ordered opal  
13 structure in which numerous recognition sites were created during imprinting. The PNP  
14 recognition swelled the colloidal spheres, leading to a red shift of the diffraction wavelength  
15 of the CCA due to the lattice spacing change and the effective diffractive index change. The  
16 relationship between the diffraction wavelength of the CCA and the size of the colloidal  
17 spheres were studied and the size of the molecularly imprinted colloidal spheres was  
18 optimized to 200 ( $\pm 5$ ) nm by adjusting the recipe composition during the emulsifier-free  
19 emulsion polymerization. As a result, color change due to the diffraction light shift which is  
20 related to PNP concentrations can be observed. The results showed that the diffraction  
21 wavelength of the molecularly imprinted colloidal array (MICA) red-shifted more than 50 nm

22 in response to 30 mM of PNP with a detection limit of 1 mM PNP. The color change of the  
23 MICA from green to red was observed. The imprinting efficiency of the molecularly  
24 imprinting, the effect of buffer pH and the selectivity were also investigated. We achieved a  
25 facile colorimetric detection method for PNP without sample treatment.

26 Keywords: photonic crystal, molecular imprinting, colorimetric detection, crystalline colloidal  
27 array

## 28 1 Introduction

29 As an endocrine disrupting compound (EDC), *p*-nitrophenol (PNP) has harmful effects for  
30 public health [1, 2]. Methods have been developed for the detection of PNP in water. As  
31 described in the literature, solid-phase extraction [3] and high-performance liquid  
32 chromatography (HPLC) [1] have been applied for the analysis of PNP in water as well as an  
33 on-line method using solid-phase extraction coupled to supercritical fluid chromatography[4].  
34 In addition, thin layer chromatography [5] and an interfaced plasma chromatograph/mass  
35 spectrometer technique[6] have been reported for the detection of phenolic pollutants.  
36 Generally, these methods need special instruments or time-consuming and laborious sample  
37 derivation. Therefore, it is still useful and highly desirable to develop a new, convenient  
38 method for detecting PNP and other EDCs.

39 Photonic crystals exhibit unique structural color on the basis of Bragg diffraction if the lattice  
40 spacing is appropriate [7, 8]. Responsive photonic crystals (RPCs) with properties that can be  
41 tuned by external stimuli have important applications as biological and chemical sensors  
42 [9-11]. Molecular imprinting is a well-established technique for the preparation of highly  
43 selective polymers with specific recognition ability [12, 13]. To improve the selectivity of  
44 RPCs, Li et al. coupled molecular imprinting with photonic crystals to create self-reporting  
45 specific sensors that detect proteins, medicines and biomarkers [14-16]. Our group also  
46 prepared molecularly imprinted photonic crystals to detect glucose and nerve agents [17, 18].  
47 Most RPCs mentioned above have a three dimensional (3D), interconnected porous, inverse  
48 opal structure within a hydrogel matrix formed by crystalline colloidal array (CCA)

49 templating methods. However, formation of high-quality RPCs with inverse opal structure  
50 over a large area usually takes hours, days, or even months to complete, and the wet etching  
51 of the crystal template may also destroy the hydrogel matrix. Imprinted template molecules  
52 must be washed away from the fragile inverse opal, which may further destroy the hydrogel.  
53 Thus, fabrication difficulties have provided a major driving force to develop alternative  
54 approaches to classic, inverse opal RPCs.

55 Most recently, our group first reported on a molecularly imprinted colloidal array prepared by  
56 combining photonic crystal and molecular imprinting technique to detect PNP [19]. This  
57 proof of principle sensor was fabricated by a self-assembly approach using molecularly  
58 imprinted colloidal spheres with a diameter of 280. In aqueous solution, PNP swelled the  
59 imprinted colloidal spheres, which increased the lattice spacing, thus shifted the diffraction  
60 wavelength. The advantage of this approach is that the imprinted colloidal spheres act both as  
61 a recognition element which recognizes the target molecule, and as a signal transfer element  
62 which causes the diffraction shift. Usually, the ordered array of an opal crystalline colloidal  
63 array collapses easily in aqueous solution. To prevent the destruction of the CCA, we  
64 stabilized the ordering of the CCA with adhesive tape. This preliminary work confirmed the  
65 feasibility of the concept described above; however, it was only primary efforts without  
66 complete characterization. First, the original diffraction wavelength (without PNP in aqueous  
67 solution) of the molecularly imprinted colloidal array (MICA) was out of visible color region  
68 (more than 770nm), which is not appropriate for a colorimetric sensor if it further red shifts.  
69 Secondly, the optical response mechanism of diffraction wavelength red shift has not been

70 fully understood. In addition, the PNP sensing environment effect, such as pH, reusability of  
71 the sensor was not investigated neither.

72 Herein, as an improvement of our previous work and further demonstration that the developed  
73 principle is applicable for colorimetric detection, we report in full detail for the designing and  
74 synthesis of a MICA film as a visible indicator for PNP in surface water. The procedure to  
75 prepare our photonic crystal sensor is easier than previous inverse RPCs as described above.  
76 MICAs with the diffraction wavelength in visible light region were fabricated and exhibit a  
77 selective PNP colorimetric indicator. The swelling of the colloidal spheres due to PNP  
78 recognition increases the lattice spacing and the filling factor of the CCA both red shift the  
79 diffraction wavelength. The effect of pH, the reusability and some surface water detection  
80 using the MICAs were finally investigated.

## 81 **2 Experimental**

### 82 **2.1 Materials**

83 *p*-Nitrophenol (PNP), *m*-nitrophenol (MNP), *o*-nitrophenol (ONP), phenol, 3-aminophenol  
84 (3-AP), sulfuric acid and hydrogen peroxide (30% water solution) were purchased from China  
85 National Medicines Co. Ltd and used as received. Methyl methacrylate (MMA), acrylamide  
86 (AM) and potassium peroxydisulfate was purchased from Xilong Chemical Co. Ltd. MMA  
87 was purified by passing through an Al<sub>2</sub>O<sub>3</sub> column before usage. Methanol (HPLC grade) was  
88 purchased from Yuwang Industrial Co. Ltd. All solvents and chemicals are of reagent quality  
89 and were used without further purification unless specially described.

90 Glass slides (50×24×0.12 mm) were obtained from Weiss Experiment Products Co. Ltd,  
91 China. Before use, glass slides were immersed in H<sub>2</sub>SO<sub>4</sub>/H<sub>2</sub>O<sub>2</sub> mixture (7:3) for 12 h, and  
92 then rinsed with deionized water in ultrasonic bath three times. Adhesive tape was obtained  
93 from Deli Stationery, China.

## 94 **2.2 Preparation of PNP imprinted colloidal spheres**

95 Monodisperse PNP imprinted colloidal spheres were prepared by emulsifier-free emulsion  
96 polymerization using a four-neck round-bottom flask which contained a reflux condenser, and  
97 a Teflon stirrer, powered by a mechanical stirrer. The flask also contained a temperature  
98 sensor and a nitrogen inlet. The reaction flask was charged with 255 mL of pure water  
99 containing varying amounts of MMA, AM and PNP. A nitrogen atmosphere and a stirring  
100 rate of 300 rpm were maintained throughout the reaction. This solution was deoxygenated by  
101 bubbling with nitrogen for half an hour. After thorough deoxygenation, the temperature was  
102 increased to 80±1 °C, and a solution of 0.6g potassium peroxydisulfate in 15 mL water was  
103 injected. The reaction was left to reflux for 45 min. After polymerization, the monodisperse  
104 PNP imprinted colloidal spheres were separated from the resulting emulsion by centrifugation  
105 at 5500 rpm for 5min. To remove the template molecules, imprinted colloidal spheres were  
106 then washed with acetic acid/methanol/deionized water (1:4:5, v/v), methanol/deionized water  
107 (1:1, v/v) and deionized water respectively. As a control experiment, non-imprinted colloidal  
108 spheres were also prepared in the same manner in the absence of PNP.

## 109 **2.3 Formation of MICA films**

110 The monodisperse PNP imprinted colloidal spheres were fully dispersed in deionized water  
111 (0.25-0.35 wt %) and then were added into a clean Petri dish. Clean glass slides were placed  
112 vertically into a Petri dish to allow colloidal crystal array growth. After complete evaporation  
113 of deionized water, MICAs were formed on both sides of each glass slide and then transferred  
114 to an adhesive tape.

#### 115 **2.4 Characterization of imprinted colloidal spheres and MICA**

116 Binding isotherms were measured to determine the adsorption capacity of imprinted colloidal  
117 spheres. PNP (0.1-1.5 mg mL<sup>-1</sup>) prepared in 1.0 mL methanol: deionized water (6:4, v/v) was  
118 incubated with 10 mg imprinted colloidal spheres for 1 h at room temperature. After  
119 incubation and separation of the colloidal spheres by centrifugation, the residual  
120 concentration of PNP in the supernatant was determined by HPLC (Shimadzu LC-20A HPLC  
121 system) with a SPD-20A UV detector. A 250 × 4.6 mm Promosil C8 analytical column  
122 (Agela Technologies) was used. Methanol-water (5.5:4.5, v/v) was used as the mobile phase  
123 at 1 mL min<sup>-1</sup>. The injection volume was 20 μL and the UV detection wavelength was 260 nm.  
124 The isotherms and the capacity were obtained by the regression of adsorption data using  
125 Prism (GraphPad Software, Inc.).

126 The reflection of the MICA was recorded using an Avaspec-2048TEC UV/Vis spectrometer  
127 with an AvaLight-DH-S-BAL light source and a FC-UV600-2-SR fiber optic reflection probe.  
128 The MICA films were equilibrated in deionized water before recording reflection  
129 measurements. The MICA films were cut to 5 mm × 5 mm and incubated in phosphate buffer



130 (pH = 6.0, 0.04 M) for 5 min before each UV-vis scan, and were then incubated into 0-30 mM  
131 PNP solutions respectively. After detection, the film was rinsed with a methanol/water (1:1,  
132 v/v) solution 3 times for recovery.

133 The color changes of the MICA films were photographed using a common digital camera  
134 under a daylight lamp. After sputter coating the MICA with a thin layer of Au, the size and  
135 morphology was examined using Scanning Electron Microscopy (S-4800, HITACHI).

### 136 **3 Results and discussion**

#### 137 **3.1 Preparation of MICA**

138 Figure 1a displays the experimental procedure employed for the construction of PNP MICA,  
139 including the polymerization of imprinted colloidal spheres, the self-assembly of the CCAs,  
140 and the stabilization of the CCAs by using an adhesive tape.

141 Firstly, monodisperse PNP imprinted colloidal spheres with a diameter of 200 ( $\pm 5$ ) nm were  
142 synthesized by emulsion-free polymerization. The size of the PNP imprinted colloidal spheres  
143 can be tuned in the range of 150 to 280 nm by changing the polymerization conditions. After  
144 removing the PNP, recognition sites were created inside the colloidal spheres. Due to the  
145 non-covalent bonds between PNP and functional monomer MMA and AM, these recognition  
146 can recognize PNP specifically. Secondly, highly ordered close-packed MICA was prepared  
147 by a vertical deposition method on glass substrates. During the MICA formation, constant  
148 temperature (30°C) and humidity (50%) were necessary to produce a highly ordering MICA  
149 with minimum defect. It should be noted that the MICAs on the surfaces of the glass slides

150 lack stability when incubated in aqueous solutions and cannot be used in practical  
151 applications. Thermal treatment has been used to stabilize CCAs on glass slides [20], but the  
152 colloidal spheres melt at high temperature. CCAs can be imbedded inside a hydrogel matrix  
153 [10, 14, 21], however, infiltration of hydrogel precursor solution may also destroy the crystal  
154 array. Thus, in our case, the MICAs were stabilized by being transferred from glass substrates  
155 to an adhesive tape. Once stuck to adhesive tape for stabilization, MICA films showed good  
156 physical stability. The MICAs on adhesive tapes exhibited bright structural color. Figure 1b  
157 shows the MICA with 200 nm colloidal spheres on adhesive tape with green structure color.

### 158 **3.2 Optimization of the size of colloidal spheres**

159 For a close-packed CCA, the diffraction wavelength of CCA changes as the size of colloidal  
160 sphere changes which results in the alterations of CCA lattice constant. In order to prepare  
161 MICAs with a desired visible structural color, PNP imprinted colloidal spheres with diameters  
162 of 150 nm, 200 nm, 250 nm and 280 nm were prepared using the recipes listed in Table 1. It  
163 was found that the average size of the colloidal spheres can be adjusted by changing the  
164 reaction parameters including the amount of monomers and initiator, temperatures, and  
165 rotation speed. Herein, the colloidal spheres with different diameters were obtained by  
166 varying the amount of monomers. After polymerization, PNP was washed off by organic  
167 solvents, leaving the monodisperse PNP imprinted colloidal spheres. As a control experiment,  
168 non-imprinted colloidal spheres were also prepared in the same manner in the absence of  
169 PNP.

170 All of these imprinted colloidal spheres with diameters of about 150 nm, 200nm, 250nm and  
171 280nm readily form close-packed CCAs by a vertical deposition method, which strongly  
172 diffract light of a specific visible wavelength. SEM images of the MICAs fabricated by  
173 different sized spheres are displayed in Figure 2. As shown in Figure 2, the colloidal particles  
174 were arranged into a 3D close-packed face-centered cubic (FCC) structures through  
175 self-assembly. On the other hand, the highly ordered periodic opal structure of the MICA  
176 leads to highly specific surface areas, which enabled them rapidly and sensitively respond to  
177 target analytes.

178 For photonic crystals with FCC structure, the maximum diffraction wavelength follows  
179 Bragg's Law (1),

$$180 \quad m\lambda = 2n_{\text{eff}}d \sin \alpha \quad (1)$$

181 where  $m$  is the diffraction order,  $\lambda$  is the wavelength of the diffracted light,  $n_{\text{eff}}$  is the effective  
182 refractive index of the CCA,  $d$  is the interplanar spacing, and  $\alpha$  is the angle of incidence.  
183 Because of the close-packed CCA in this study, the diffraction wavelength  $\lambda$  could be varied  
184 by changing the diameter of the colloidal spheres. The prepared 150, 200, 250, and 280 nm  
185 MICAs diffracted 370, 509, 630, and 756 nm at normal angle respectively (Figure 3a), and  
186 different structural colors were observed. As we can see in Figure 3b, the diffracted  
187 wavelengths of 200 and 250 nm MICAs lie in visible light region, green and red colors are  
188 observed. However, MICAs containing 150 and 280 nm colloidal spheres diffracted UV and  
189 near infrared light respectively. No structural color could be observed for 150 nm MICA. It

190 can be seen that 280 nm MICA shows violet structural color even though the diffracted  
191 wavelength is out of visible region. This structural color could be attributed to the second  
192 order diffraction of the MICA. For MICAs containing 250 nm colloidal spheres, there would  
193 be no significant color change for any further red shift, because it diffracts red light. Thus, the  
194 colloidal spheres with a diameter of 200 nm were selected for the following investigations.

### 195 **3.3 Sensing properties of MICA**

196 MMA and AM were chosen as functional monomers for the recognition of PNP. The binding  
197 capacities of PNP on the molecularly imprinted colloidal (MIC) spheres were analyzed, and  
198 the results are shown in Figure 4a. It was observed that the adsorption amount of PNP on the  
199 imprinted colloidal spheres increased with an increasing PNP concentration. The adsorption  
200 capacity was approached equilibrium at the high concentration. This result suggested that the  
201 imprinted spheres possessed a large number of specific binding sites within the colloidal  
202 spheres. The adsorption capacity of imprinted spheres to PNP can be calculated according to  
203 binding isotherm as  $331 \mu\text{mol g}^{-1}$ , while for the non-imprinted colloidal (NIC) spheres the  
204 adsorption capacity is  $84 \mu\text{mol g}^{-1}$ . Imprinting effect, defined as the ratio of the capacities  
205 between imprinted colloidal spheres and non-imprinted colloidal spheres, is 3.4. A  
206 satisfactory imprint was achieved.

207 The traditional molecular imprinting technique only affords thousands to millions highly  
208 specific binding pockets or recognition elements that possess the ability to recognize specific  
209 target molecules. As a sensing element, the integration of these recognition elements with an

210 appropriate transduction element is required. In our case, due to the 3-D ordered CCA  
211 structure, the signal can be generated by the MICA itself through Bragg diffraction, and the  
212 molecular recognition process can be directly transferred into readable optical signals.

213 The sensing response of the MICA to PNP was examined in phosphate buffer solution  
214 (pH=6.0, 0.04 M). Figure 4b shows the sensing behavior of the MICA fabricated by using the  
215 200 nm imprinted colloidal spheres. With an increasing of the concentration of target  
216 molecules, the diffraction peak red shifted gradually. Within 5 min, the wavelength increased  
217 from 613 to 668 nm when PNP increased to 30 mM. The color changes that accompany the  
218 peak shift of the Bragg diffraction also are visually evident. The MICA film in the phosphate  
219 buffer solution shows green color at the beginning. After the exposure to 10 mM and 30 mM  
220 PNP solution, the MICA film changed color to yellow and red, respectively (Figure 4c). For a  
221 better comparison, diffraction wavelength shifts vs. PNP concentration were plotted instead of  
222 the raw data (Figure 4d). Notably, this selective detection is relatively sensitive for PNP, as  
223 evident from the detection of 1 mM PNP solution. Compared with the detection limit of  
224 0.2mg/L of traditional PNP detection method based on HPLC or Mass spectroscopy [1,3], the  
225 detection limit of MICA is still needed to improve. However, these traditional methods  
226 involve time-consuming sample preparation and expensive instruments. Our MICA provides  
227 a simple way and colorimetric detection for PNP. As a control experiment, a non-imprinted  
228 colloidal array (NICA) film with the same photonic structure was also constructed (Figure 4d).  
229 It exhibited only a minor shift when it was soaked in PNP solutions with the same  
230 concentration variation as the MICA film described above (Figure 4b). Although the detection

231 method based on the MICA is actually semi-quantitative, it did offer us a facile colorimetric  
232 detection method.

### 233 3.4 Sensing principles

234 This selective sensing mechanism can be attributed to the hydrogen bond interactions,  
235 electrostatic attraction and associated weak interactions between the target molecules of PNP  
236 and functional monomers. The target molecule and the specific binding sites of MICA  
237 produced a specific recognition by noncovalent bonds, and the process of recognition can  
238 swell the spheres. With increasing PNP concentration, the size of spheres increased, and  
239 results in an increase in the interplanar spacing followed by a reflection peak red shift (Figure  
240 5a). Furthermore, the increase in the effective refractive index can be one of the factors  
241 causing the diffraction peak red shift. The hydrophilic functional comonomer AM makes the  
242 exterior of the colloidal spheres more flexible and soft [22]. In response to PNP adsorption,  
243 swelling of imprinted colloidal spheres caused the space between colloidal spheres to become  
244 occupied (Figure 5b). Thus, the filling factor of the CCA increases. The effective refractive  
245 index  $n_{\text{eff}}$  of the crystal is calculated as follows [23]:

$$246 \quad n_{\text{eff}} = \sqrt{f \cdot n_m^2 + (1-f)n_v^2} \quad (2)$$

247 Where  $f$  is the filling factor,  $n_m$  is the refractive index of the colloidal spheres, and  $n_v$  is the  
248 refractive index of the voids. In this research,  $n_v$  is the refractive index of the PNP solution  
249 and below the value of  $n_m$ . Once the voids are occupied, the filling factor increased, and the  
250  $n_{\text{eff}}$  increased, eventually leading to the red shift of the reflection peak. According to Figure

251 5b, colloidal spheres swelled by about 10% in response to 20 mM PNP. The results in our  
252 research suggest that a close-packed MICA can swell in response to analytes and show a  
253 visual optical signal.

### 254 **3.5 Response characteristics and reproducibility**

255 To optimize the response of the MICA, the red shift of reflectance in response to 10mM PNP  
256 under different pH conditions was investigated (Figure 6a). Most PNPs ( $pK_a=7.16$ ) [24] exist  
257 as anions when the solution  $pH > pK_a$ , and as a neutral molecule when the solution  $pH < pK_a$ .  
258 As the pH of the PBS decreases, more and more PNP exists as its neutral molecule structure.  
259 When the pH value is too low in solution, more  $H^+$  may affect the hydrogen bond between the  
260 PNP and the AM, leading to less PNP adsorption by the imprinted colloidal spheres.  
261 Generally, the experiment results showed that at  $pH=5$  and  $pH=6$ , MICAs had better optical  
262 responses to the target. The selectivity test of the MICA was carried out by using its  
263 analogues, phenol, *m*-nitrophenol (MNP), *o*-nitrophenol (ONP) and 3-aminophenol (3-AP). It  
264 was seen that there were almost no diffraction wavelength changes in response to phenol,  
265 ONP, and 3-AP. The red reflection of the MICA shifted significantly in response to MNP,  
266 which has similar structure to PNP (Figure 6b). The reusability of the MICA was evaluated  
267 by an elution and rebinding method. From Figure 6c, it can be observed obviously that MICA  
268 possessed an ideal recoverability within five cycles and the standard error was just within 5%.

269 To test the possibility of utilizing the MICA to colorimetrically detect PNP from  
270 environmental samples, the MICA film was subjected to surface (from the Linglong Lake,

271 Beijing, China) and tap waters (Beijing, China) spiked with PNP. The results showed that the  
272 reflectance peak, in surface and tap water, shifted approximately 55 nm and 50 nm,  
273 respectively, towards 30 mM PNP. The color of the MICAs changed from green to red  
274 (Figure 7). A relative linearity of the response of the MICA to 1 to 30 mM PNP from surface  
275 and tap water is observed ( $r^2=0.971$  and  $0.985$ , respectively), and a LOD of 1 mM was  
276 achieved.

#### 277 **4 Conclusions**

278 In summary, a simple and low cost colorimetric method to detect PNP was developed by  
279 self-assembling imprinted colloidal spheres into a close-packed CCA structure. Adhesive tape  
280 can be used to stabilize the CCAs. The result shows that the imprinted CCA has high  
281 selectivity and great regenerating ability in an aqueous environment. More importantly,  
282 MICA directly generates colorimetric signals, which is suitable for reporting recognition  
283 events without any necessary treatments of analytes. It is envisaged that the MICA could  
284 provide a promising alternative to current methods of onsite monitoring of PNP levels.

#### 285 **5 Acknowledgments**

286 This work was supported by the NSFC (20775007), 863 project (2007AA10Z433) and  
287 SKLECC (KF0908). Scientific advice from Professor Sanford Asher from Department of  
288 Chemistry, University of Pittsburgh is appreciated.

289 References



- [1] R. Belloli, B. Barletta, E. Bolzacchini, S. Meinardi, M. Orlandi, B. Rindone, *Journal of Chromatography A*, 846 (1999) 277.
- [2] M. Janotta, R. Weiss, B. Mizaikoff, O. Bruggemann, L. Ye, K. Mosbach, *International Journal of Environmental Analytical Chemistry*, 80 (2001) 75.
- [3] E. Caro, R.M. Marcé, P.A.G. Cormack, D.C. Sherrington, F. Borrull, *Journal of Chromatography A*, 995 (2003) 233.
- [4] E. Pocurull, R.M. Marcé, F. Borrull, J.L. Bernal, L. Toribio, M.L. Serna, *Journal of Chromatography A*, 755 (1996) 67.
- [5] R.L. Bamberger, J.H. Strohl, *Analytical Chemistry*, 41 (1969) 1450.
- [6] F.W. Karasek, S.H. Kim, H.H. Hill, *Analytical Chemistry*, 48 (1976) 1133.
- [7] J.D. Debord, L.A. Lyon, *The Journal of Physical Chemistry B*, 104 (2000) 6327.
- [8] G.I.N. Waterhouse, M.R. Waterland, *Polyhedron*, 26 (2007) 356.
- [9] J. Ge, Y. Yin, *Angewandte Chemie International Edition*, 26 (2010) 18357.
- [10] J.H. Holtz, S.A. Asher, *Nature*, 389 (1997) 829.
- [11] D. Nakayama, Y. Takeoka, M. Watanabe, K. Kataoka, *Angewandte Chemie-International Edition*, 42 (2003) 4197.
- [12] G. Wulff, *Angewandte Chemie International Edition in English*, 34 (1995) 1812.
- [13] C. Alexander, H.S. Andersson, L. I. Andersson, R. J. Ansell, N. Kirsch, I. A. Nicholls, J. O'Mahony, M. J. Whitcombe, *Journal of molecular recognition*, 19 (2006) 106.
- [14] X. Hu, Q. An, G. Li, S. Tao, J. Liu, *Angewandte Chemie International Edition*, 45 (2006) 8145.
- [15] X.B. Hu, G.T. Li, J. Huang, D. Zhang, Y. Qiu, *Advanced Materials*, 19 (2007) 4327.
- [16] X.B. Hu, G.T. Li, M.H. Li, J. Huang, Y. Li, Y.B. Gao, Y.H. Zhang, *Advanced Functional Materials*, 18 (2008) 575.
- [17] F. Xue, T.-R. Duan, M. Xue, F. Liu, Y.-F. Wang, Z.-Q. Wei, M. Wang, P. Zhang, Z.-G. Yuan, Z.-H. Meng, *Chinese Journal of Analytical Chemistry*, 39 (2011) 1015.
- [18] F. Liu, S. Huang, F. Xue, Y. Wang, Z. Meng, M. Xue, *Biosensors and Bioelectronics*, 32 (2012) 273.
- [19] F. Xue, Y.-F. Wang, Q.-H. Wang, Z.-H. Meng, M. Xue, S.-Y. Huang, W. Lu, *Chinese Journal of Analytical Chemistry*, 40 (2012) 218.
- [20] Y. Zhu, Y. Cao, Z. Li, Y. Wang, J. Ding, J. Liu, Y. Chi, *Journal of Jilin University (Science edition)*, 45 (2007) 82.
- [21] Y. Liu, Y. Zhang, Y. Guan, *Chem Commun (Camb)* (2009) 1867.
- [22] D. Suzuki, J.G. McGrath, H. Kawaguchi, L.A. Lyon, *The Journal of Physical Chemistry C*, 111 (2007) 5667.
- [23] L. González-Urbina, K. Baert, B. Kolaric, J. Pérez-Moreno, K. Clays, *Chemical Reviews*, 112 (2011) 2268.
- [24] Q. Zhou, H.P. He, J.X. Zhu, W. Shen, R.L. Frost, P. Yuan, *Journal of Hazardous Materials*, 154 (2008) 1025.

Table 1 Recipes and diameters of imprinted colloidal spheres

Sample	Diameters (nm)	MMA (ml)	AM (mmol)	PNP (mmol)
A	280	30	15	5
B	250	24	12	4
C	200	12	6	2
D	150	6	3	1

**Figures**

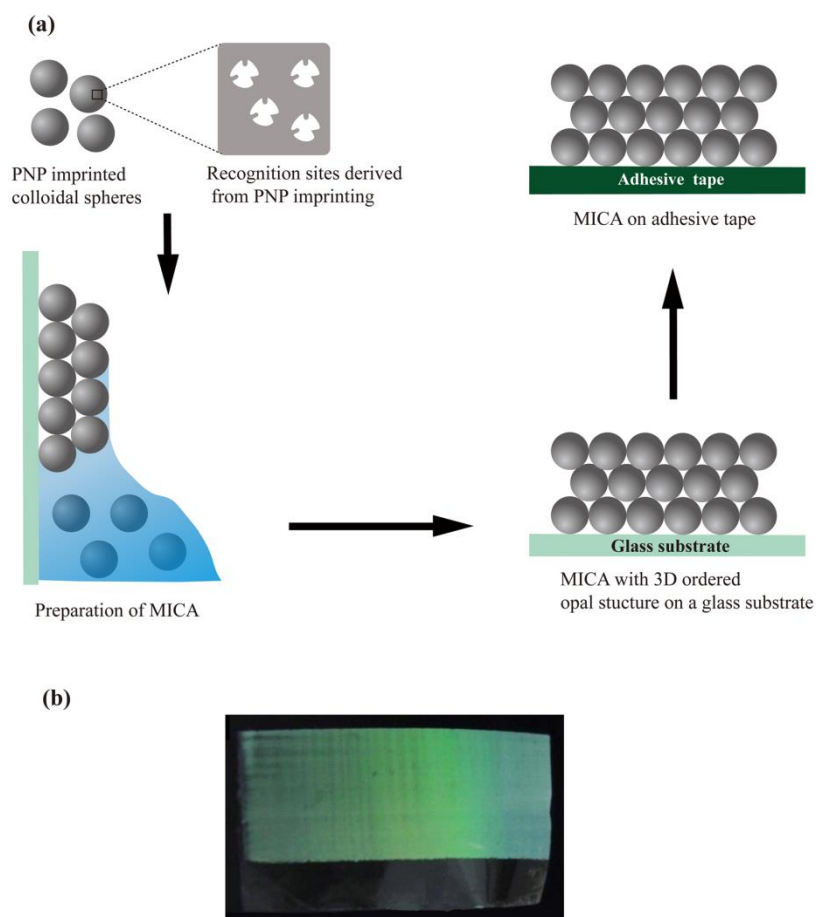


Figure 1. (a) Schematic illustration of MICA fabricating. Monodisperse PNP imprinted colloidal spheres were self-assembled into a 3-D ordered opal CCA structure on a glass substrate. Then the MICA was transferred onto an adhesive tape which conserving the intact opal structure. (b) Photograph of the MICA self-assembled by 200 nm colloidal spheres on adhesive tape with green structural color.

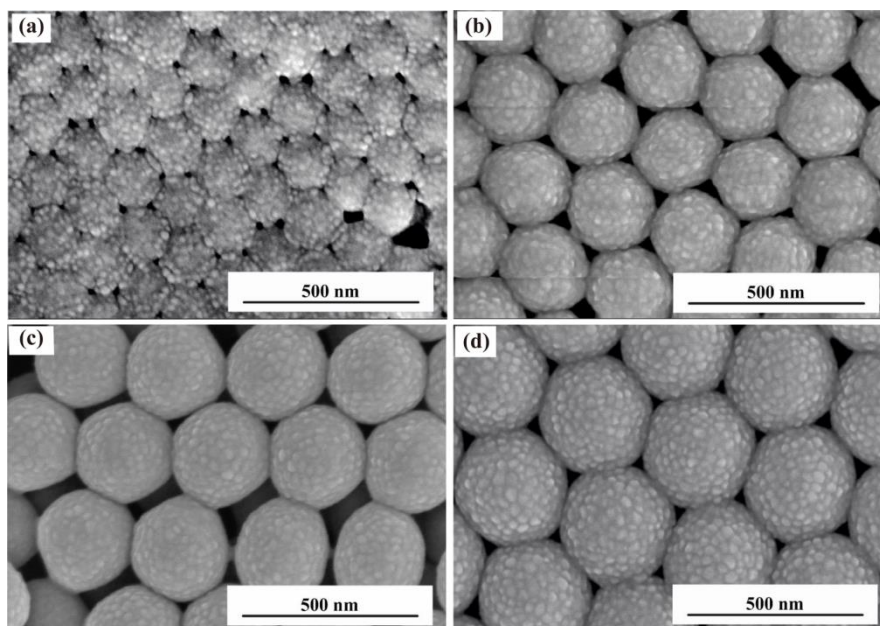


Figure 2. (a) SEM images of close-packed MICAs of different sizes, (a) 150 nm, (b) 200 nm, (c) 250 nm, and (d) 280 nm.

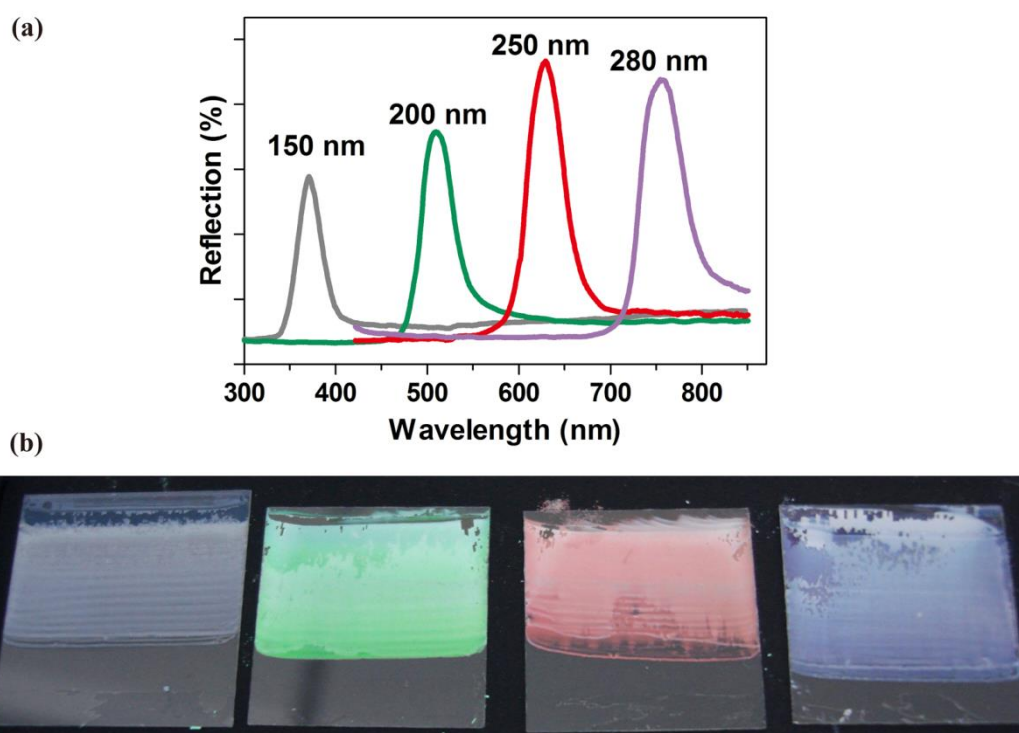


Figure 3. (a) Reflection spectra of MICAs self-assembled from different size of colloidal spheres. (b) Colors of the MICAs self-assembled from colloidal spheres with different size.

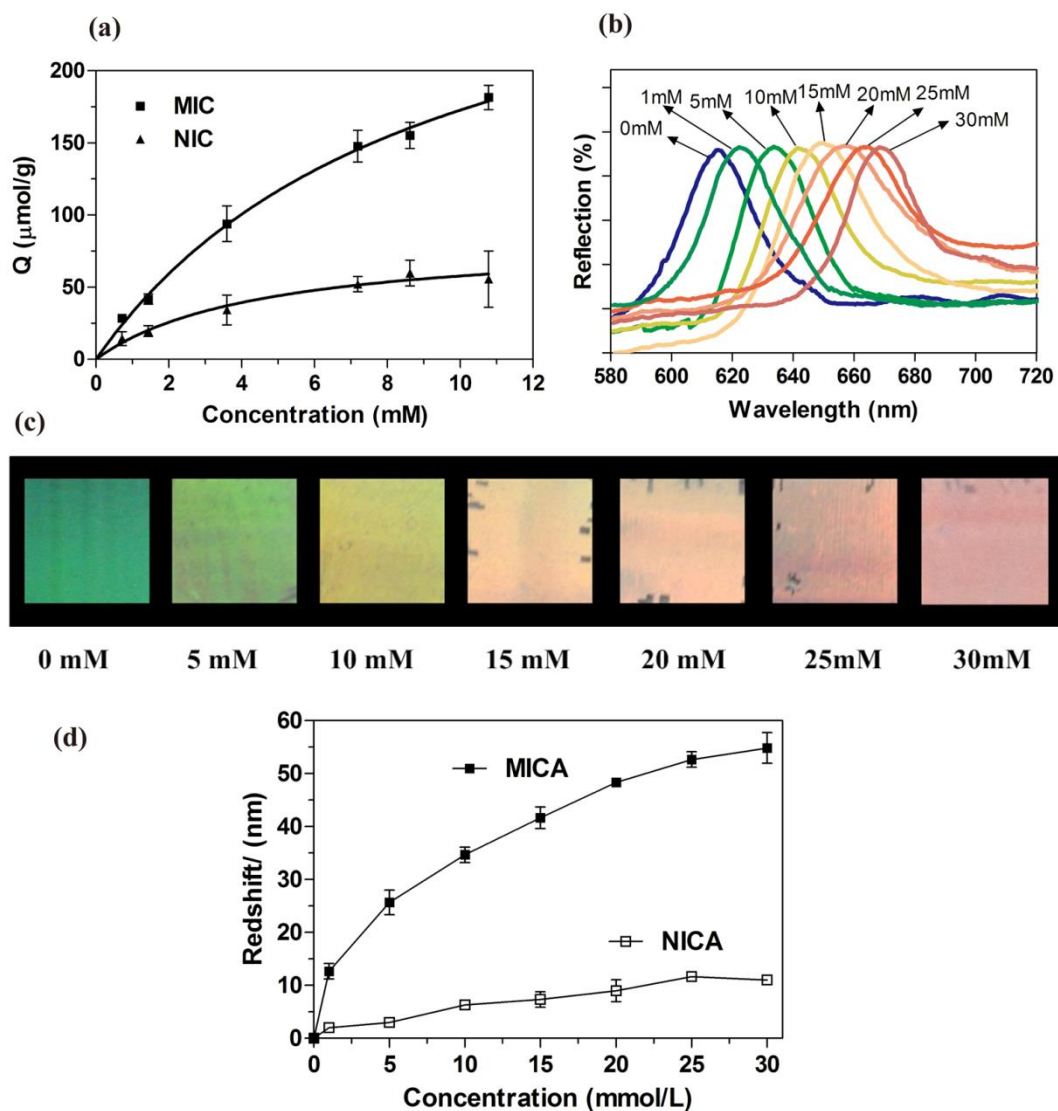


Figure 4. (a) Adsorption isotherms of PNP on imprinted colloidal spheres and non-imprinted colloidal spheres. (b) Optical response of MICA in response to PNP in phosphate buffer (pH=6.0, 0.04 M). (c) The induced color changes of the MICA film upon adsorption of PNP at different concentrations. (d) Plot of the Bragg diffraction shifts of the MICA and NICA in response to the PNP.

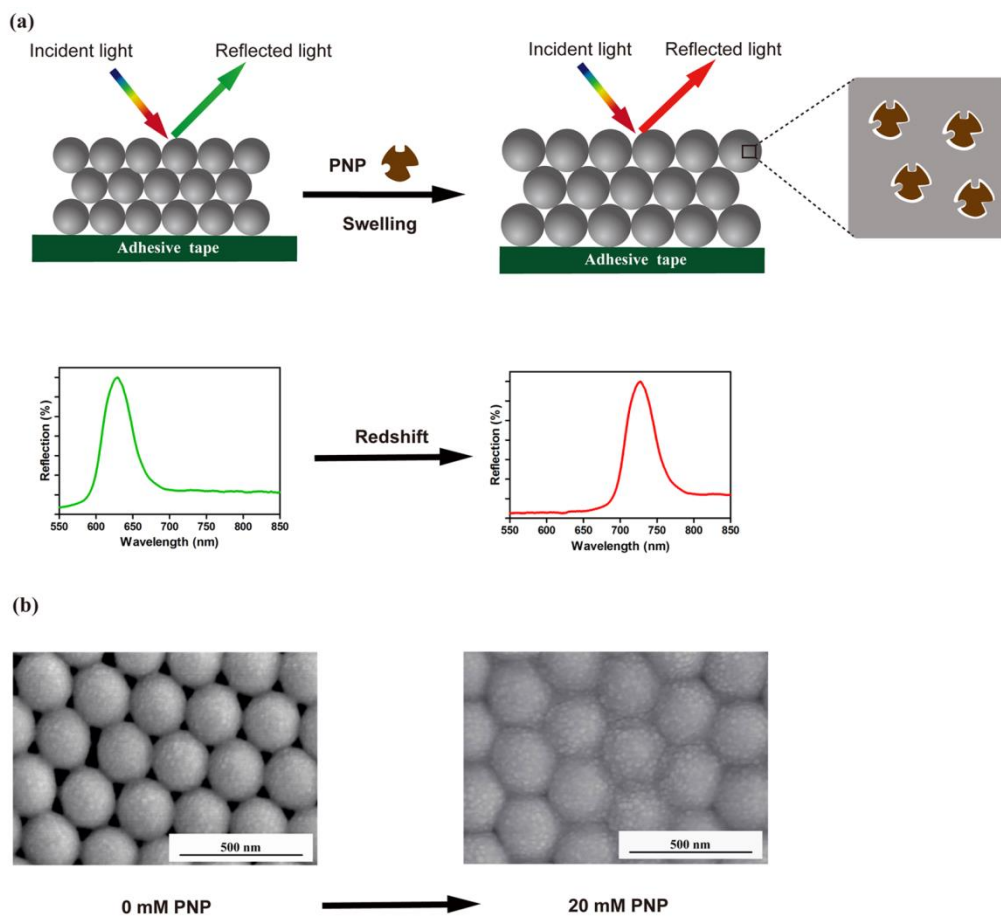


Figure 5. (a) Sensing principle of the MICA film. (b) SEM images of the MICA before and after adsorption of PNP.

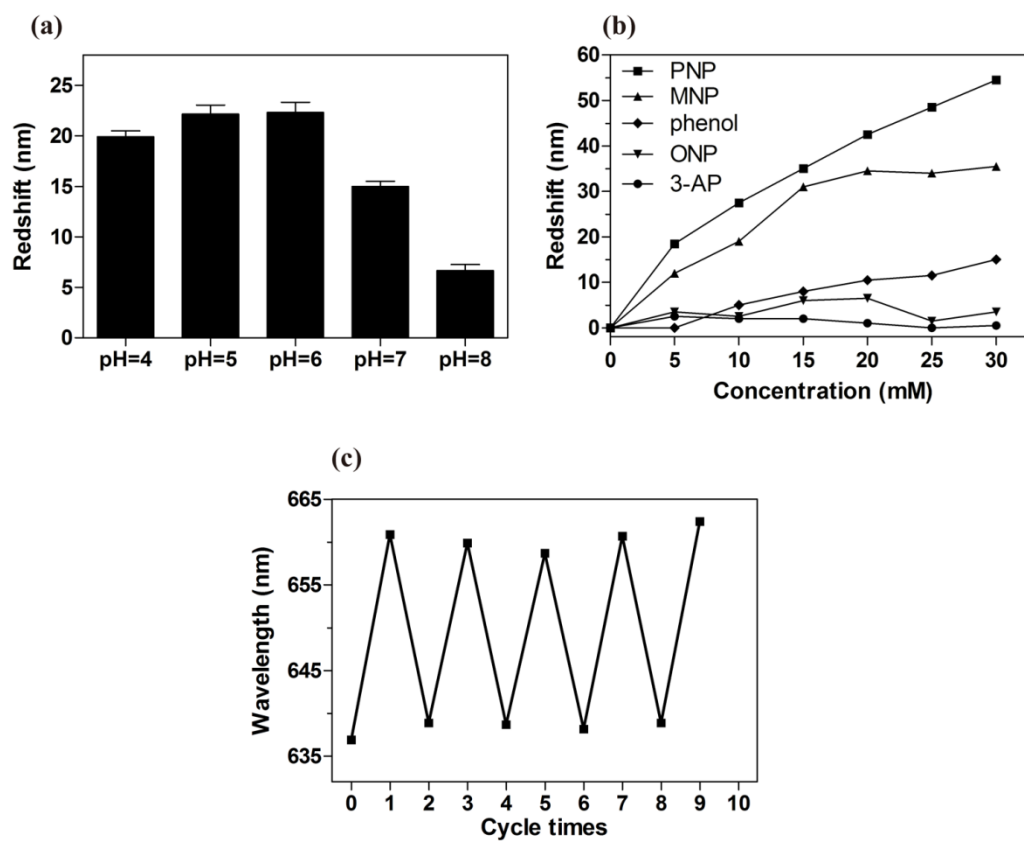


Figure 6. (a) The red shift of the MICA film in response to 10 mM PNP in phosphate buffer under various pH. (b) Red shift of MICA film in response to PNP and its analogues. (c) Recoverability of the MICA film incubated in a 10 mM PNP buffer and then recovered in a methanol/water (1:1, v/v) solution.

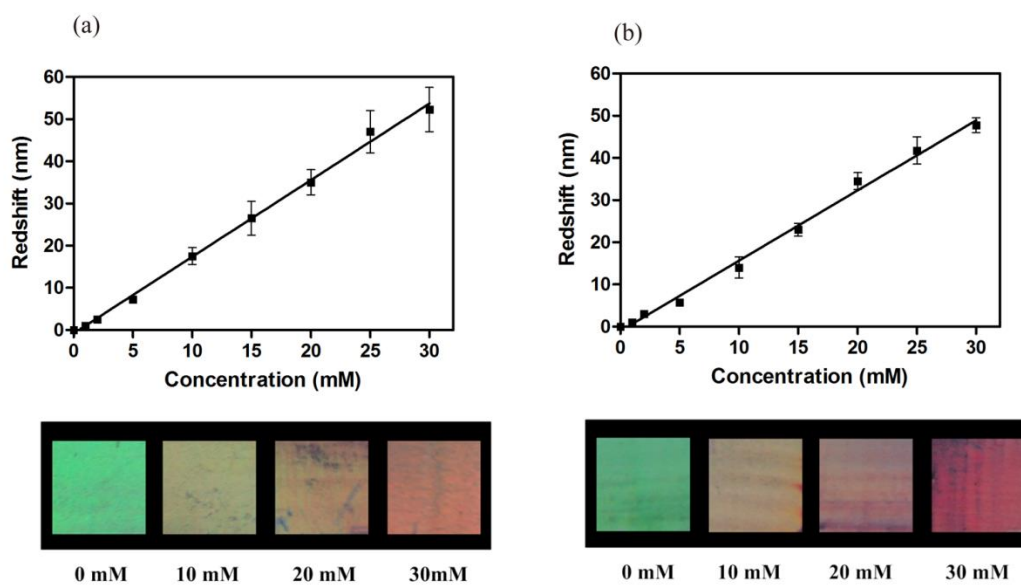


Figure 7. Reflection red shift of the MICA in response to various concentrations of PNP and their color changes in (a) surface water (from the Linglong Lake, Beijing, China) and (b) tap water (Beijing, China).